Critical Thickness of High-Temperature AlN Interlayers in GaN on Sapphire (0001)

A.M. SANCHEZ,[1] F.J. PACHECO,[1,2] S.I. MOLINA,[1] J. STEMMER,[3] J. ADERHOLD,[3] and J. GRAUL[3]

1.—Universidad de Cádiz, Departamento de Ciencia de los Materiales e I.M. y Q.I., 11510 Puerto Real, Cádiz, Spain. 2.—e-mail: paco.pacheco@uca.es. 3.—Laboratorium für Informationstechnologie, Universität Hannover, 30167 Hannover, Germany

We analyze by cross-sectional transmission electron microscopy the threading dislocation behavior when crossing an AlN intermediate layer in the GaN/AlN/GaN/sapphire system grown by molecular beam epitaxy. Dislocation behavior is explained calculating critical thickness by applying the Fischer model to an AlN layer capped with GaN. Due to elastic interaction between straight misfit dislocations, the Matthews and Blakeslee model does not explain the observed dislocation behavior. The understanding of critical thickness in the studied system permits to select the AlN interlayer thickness that minimizes the threading dislocation density in the capped GaN layer.

Key words: Transmission electron microscopy, GaN, AlN interlayers, critical thickness, threading dislocations

INTRODUCTION

Because of the wide range of applications in optical and electronic devices, III-V nitride semiconductors and their alloys have been intensively studied in recent years. The growth of GaN on the (0001) basal plane of sapphire[1,2] seems to guarantee a satisfying operation of GaN devices. Due to the large lattice mismatch and in order to avoid the formation of three-dimensional islands during the growth of GaN directly on sapphire,[3,4] different buffer layer approaches have been employed to promote uniform coverage of the GaN. Low-temperature buffer layers (LT-buffer), such as AlN[5–7] and GaN,[4–7] reduce the threading defects in the epilayer. Recently, a new approach based on the insertion of LT-GaN or LT-AlN interlayers (IL) between high-temperature GaN layers (HT-GaN) has been reported. The insertion of a high temperature AlN (HT-AlN) interlayer between the HT-GaN grown by plasma assisted molecular beam epitaxy (MBE) improves the crystalline quality through threading dislocation reduction.[9] A series of samples with different HT-AlN interlayer thickness has been characterized by transmission electron microscopy (TEM) and photoluminescence (PL). The wide number of dislocation interactions observed in the sample with intermediate HT-AlN interlayer thickness of 3.2 nm reduces the threading dislocation density reaching the GaN free surface, so that this sample presents the optimum crystalline quality.[9,10]

(Received February 7, 2001; accepted February 23, 2001)

In this paper, in order to shed some more light on this subject, we focus our study on the analysis of the effect of these HT-AlN-ILs on the threading dislocations and check the critical thickness calculated following different theoretical approaches.[11,14]

EXPERIMENTAL

GaN films with (0001)-oriented surface were grown on sapphire α-Al_2O_3(0001) substrates by plasma assisted MBE. Firstly, the sapphire substrate was covered with a 20 nm thin GaN buffer layer deposited at 520°C, followed by annealing at 750°C in order to improve the GaN film crystalline quality. A thin AlN intermediate layer (AlN-IL) was then deposited on a nominally 100 nm thick GaN layer without any growth interruption at the same temperature as GaN had been grown (685°C). This growth sequence finished with a nominally 400 nm thick GaN top layer. Two samples with AlN-IL thickness of 3.2 nm (sample S3) and 8 nm (sample S8) were grown. Further growth details on the studied samples are described in Ref. 9.

The microstructure of the layers was characterized

by conventional transmission electron microscopy in a Philips CM 20 transmission electron microscope operated at 200 kV and a Jeol 1200-EX working at 120 kV. The thickness of the AlN-IL was measured by high resolution electron microscopy (HREM) in a Philips CM300 FEG transmission electron microscope. Plan view TEM (PVTEM) specimens were thinned down to 100 μm by mechanical grinding and dimpled down to 5 μm followed by ion milling at 4.5 kV to electron transparency. Cross-sectional TEM (XTEM) samples were prepared by tripod technique. Electron transparency was achieved using a precision ion polishing system (PIPS) at 5 kV. A final step at 3kV was used to reduce ion beam damage.

PREVIOUS RESULTS ON THE EFFECT OF THE INSERTION OF AN HT-AlN INTERLAYER

In a previous report, we deduced from PL and threading dislocation density measurements by PVTEM a clear improvement of the crystalline quality by the insertion of HT-AlN interlayer.[11] The dislocations considered were those with Burgers vectors b = 1/3 <11$\bar{2}$0> and b = 1/3 <11$\bar{2}$3>. Dislocations with b = <0001> are greatly reduced during growth through half loop formations.[15] Although a small fraction of them were able to extend further away from the interface and reach the free surface, this fraction is negligible in relation to the dislocation density with an **a**-component. Wide regions of all the samples including a reference one without AlN-IL were analyzed to obtain a reliable threading dislocation densities, ρ_D, measurements. The clear reduction of ρ_D in the samples containing a HT-AlN interlayer was in good agreement with the decrease in the full width at half maximum (FWHM) of the main emission PL peaks.[9] However, the lowest value of these measurements, i.e., the better crystalline quality, was obtained for sample with the thinnest HT-AlN-IL. Preliminary XTEM studies were carried out on the full series of samples to explain the HT-AlN insertion effect on the crystalline quality. The images recorded in two beams condition with the (0002) reflection near the <11$\bar{2}$0> zone axis showed many upright threading dislocation lines across the GaN layer. However, the HT-AlN interlayer insertion causes the tilt of a few dislocation lines. This phenomenon is more frequently observed in sample S3. This leads to a higher number of threading dislocation interactions and, consequently, to a lower dislocation density reaching the sample free surface.

DISLOCATION BEHAVIOR

In this work, the dislocation behavior across the HT-AlN interlayer has been studied in detail by XTEM (Fig. 1). The influence of the AlN-IL/GaN interfaces on the threading dislocation line motion has been characterized in samples S3 and S8. As can be seen in Fig. 1 some dislocations change their dislocation line direction when reaching the AlN interface. When a threading dislocation reaches the GaN/AlN-IL interface in sample S3 the misfit strain seems not to be enough for bowing the dislocation and originate a misfit dislocation segment parallel to basal plane to accommodate the misfit at the interface. Nevertheless, stress due to the mismatch between AlN and GaN changes the threading dislocation line direction (Fig. 1a). This fact enables more interactions between threading dislocation lines. An out-standing difference between S3 and S8 samples, in addition to the higher ρ_D measured in the second one, is the dislocation line behavior reaching the AlN-IL interface. The tilt of threading dislocations is less frequent in S8 sample. Figure 1b shows the typical arrangement for threading dislocations when the epilayer thickness (AlN) exceeds a critical value. The

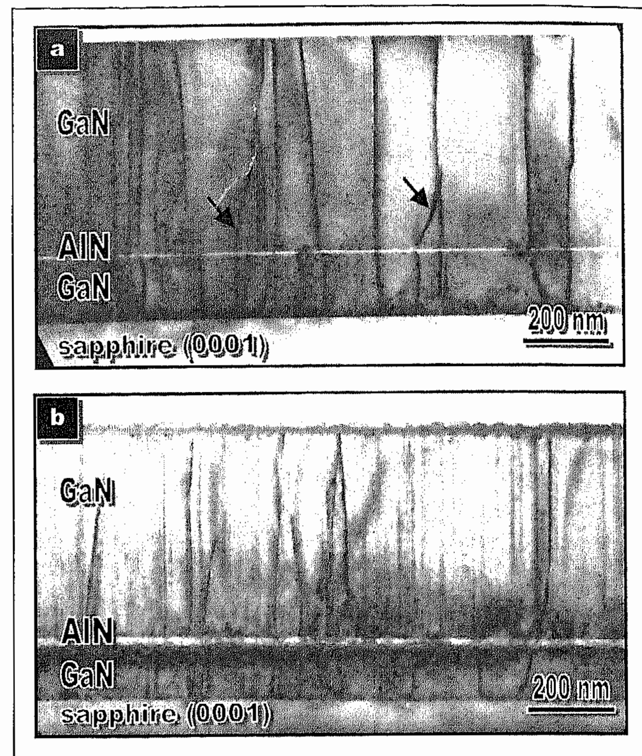

Fig. 1. Low magnification XTEM images recorded under two beam bright field condition with (0002) reflection showing dislocation lines through the (a) S3 and (b) S8 sample epilayers. Note the change of dislocation line directions in arrowed dislocations.

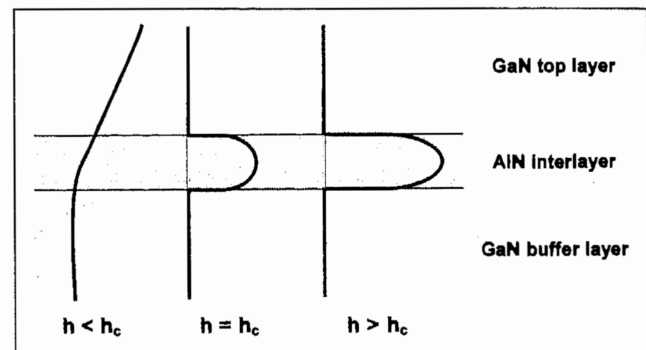

Fig. 2. Schematic drawing of the different dislocation line behaviors observed in the XTEM images.

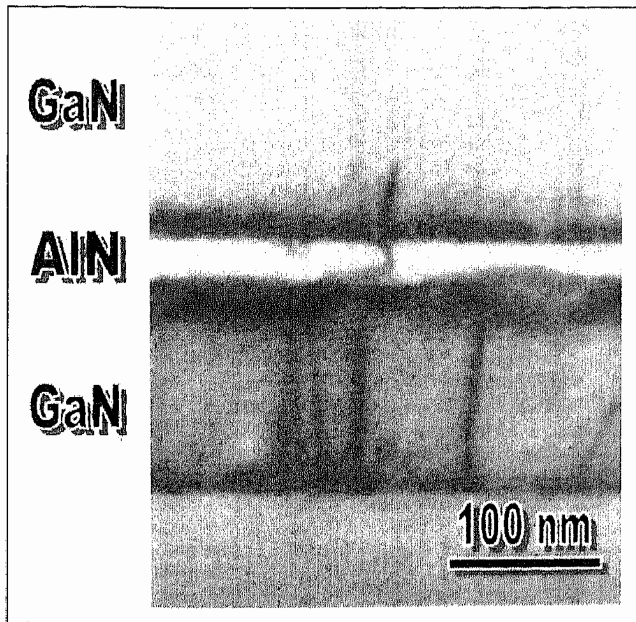

Fig. 3. XTEM micrograph showing the dislocation line bending at both GaN/AlN interfaces in sample S8.

dislocation bows because the resolved shear stress acting on the slip system is higher than the total self-stress created by the dislocation. The dislocation moves forming a half loop across the HT-AlN interlayer and continues like straight threading dislocation when leaving this region. Figure 2 shows a schematic drawing of all the observed possibilities. The threading dislocation behavior is quite different in S3 and S8 samples, as can be seen in Fig. 1. Whereas many dislocations arise bent over in sample S3, following the model showed in Fig. 2a, in sample S8, the half loops formation in the interlayer has been observed (Fig. 3b). The models represented in Fig. 2 have been checked through XTEM images recorded under two beams bright field condition like Fig. 3. The HT-AlN interlayer thickness exerts a clear influence on the dislocation line behavior and therefore on the dislocation interactions.

These different behaviors could be understood through critical thickness calculations and misfit accommodation in epitaxial multilayers. There are many different approaches for the accommodation of misfit between an epitaxial film and the substrate.

EXPLANATION OF THE OBSERVED DISLOCATION BEHAVIOR

Theoretical calculation by Matthews and Blakeslee,[11] based on thermodynamic equilibrium, is most widely used in critical thickness (h_c) studies. We estimated h_c inserting the appropriate material system AlN/GaN parameters obtaining a value of 2 nm for the Matthews and Blakeslee multilayers approach. Nevertheless, for semiconductors, equilibrium calculations supply lower values for the critical thickness than experimental observations.[12,13] Therefore, the relaxation of the elastic strain is slower than would be expected from equilibrium calculations. The Matthews and Blakeslee model ignores the phenomenon of elastic interaction between straight misfit dislocations. Here both samples present values of AlN-IL thickness measured by HREM higher than the critical one calculated following the Matthews and Blakeslee model. Nevertheless, XTEM shows that critical thickness of the AlN-IL in sample S3 has not been reached in AlN-IL of sample S3. This fact requires the use of another approach to successfully explain the dislocation behavior. Such approach is presented in the following paragraphs.

The approach developed by Fischer et al.[14] is based in the equilibrium theory including the interaction factor between straight misfit dislocations very important in systems like GaN/sapphire with dislocation densities as high as 10^{10} cm^{-2}. Previously, the validity of this approach has been successfully checked in GaN/AlN systems employing synchroton x-ray diffraction.[16] The expression for the excess resolved shear, considering an interlayer, i.e., two GaN/AlN interfaces results as follows,

$$\tau_{exc} = \tau - 2\tau_s$$

where τ represents the resolved shear stress acting on the slip system on a misfit dislocation and τ_s the shear component of the total self-stress created by the dislocation. Due to the fact that the studied samples have an AlN interlayer the double τ_s value is included in the equation. If the HT-AlN thickness is higher than the critical value, we can consider the multilayers approach, so the dislocation should bend in both interfaces between HT-GaN and HT-AlN.

Taking the equilibrium conditions for the point of strain relief onset via plastic flow leads to the following expression for the critical thickness h_c,

$$\frac{a_0 - a_1}{a_0} = \frac{b\cos\lambda}{2h_c}\left(1 + \left(\frac{1 - v\cos^2\theta}{2\pi(1+v)\cos^2\lambda}\right)\ln\left(\frac{h_c}{b}\right)\right)$$

According to L. Sugiura,[17] the dominant misfit dislocation type in wurtzite GaN system is 60 degree dislocations on (0001) plane. Thus, the most proper value for λ and θ is $\pi/6$. Inserting appropriate material system parameters, a_1 = 0.3110 nm, a_0 = 0.3189 nm, $\lambda = \pi/6$, v_{AlN} = 0.608, and b = 0.3189 nm, the calculated critical thickness of HT-AlN interlayer is 7.56 nm,' nearly four times larger than the critical thickness by the Matthews and Blakeslee model. As the first HT-GaN layer thickness grown directly over the GaN buffer layer is 100 nm or higher in both samples, fully relaxed parameters have been considered for GaN.

In this case, only the AlN interlayer thickness in the S8 sample will exceed the critical value. In previous reports,[17,18] the straight threading dislocation behavior has been described. When the film thickness exceeds the critical value, some of them change into the basal plane to become misfit segments parallel to the interface. The behavior of a threading dislocation that reaches the interface depends on the epilayer thickness.[11]

As the HT-AlN interlayer in S3 sample does not exceed the critical thickness value, threading dislocations tend to change direction when they reach the interface, and interactions between dislocations are favored as can be seen in Fig. 1a. Thus the threading dislocation density reaching the free surface in the GaN overlayer must be lower, as was checked by PL measurements and dislocation density evaluations.[9] Therefore, our experimental results are in good agreement with the calculated critical thickness in wurtzite AlN/GaN multilayer systems by applying the Fischer model.

SUMMARY

In this paper we have successfully checked the validity of the Fischer approach in systems containing a HT-AlN interlayer. The introduction of a thin HT-AlN intermediate layer in HT-GaN grown by plasma assisted MBE reduces the threading dislocation density. This reduction is higher when the HT-AlN thickness is below the critical value calculated by the Fischer model equation to a capped layer, because the bending and interactions between dislocations occur more frequently in this case.

ACKNOWLEDGEMENT

We acknowledge support from CICYT, Project MAT 98-0823, from the Junta de Andalucia under the group TEP-0120. TEM measurements were carried out using the facilities of CIME, EPFL, Lausanne, Switzerland and DME, SCCYT, University of Cádiz, Spain.

REFERENCES

1. S. Nakamura, M. Senoh, S. Nagahama, N. Iwasa, T. Yamada, T. Matsushita, Y. Sugimoto, and H. Kiyoku; *Appl. Phys. Lett.* 70, 868 (1997).
2. H. Morkoç, S. Strite, G.B. Gao, M.E. Lin, B. Sverdlov, and M. Bums; *J. Appl. Phys.* 76, 4363 (1994).
3. H. Amano, N. Sawaki, I. Akasaki, and Y. Toyoda, *Appl. Phys. Lett.* 48, 415 (1998).
4. S. Nakamura, *Jpn. J. Appl. Phys.* 30, L1705 (1991).
5. S. Yoshida, S. Misawa, and S. Gonda, *Appl. Phys. Lett.* 42, 42 (1983).
6. H. Amano, N. Sawaki, I. Akasaki, and Y. Toyoda, *Appl. Phys. Lett.* 48, 353 (1986).
7. E.C. Piquette, P.M. Bridger, R.A. Beach, and T.C. MacGill, *MRS Internet J. Nitride Semicond. Res.* 4S1, G3.77 (1999).
8. M. Iwaya, T. Takenchi, S. Yamaguchi, C. Wetzel, H. Amano, and I. Akasaki, *Jpn. J. Appl. Phys.* 37, L316 (1998).
9. J. Stemmer, F. Fedler, H. Klausing, D. Mistele, T. Rotter, O. Semchinova, J. Aderhold, J. Graul, A.M. Sanchez, F.J. Pacheco, S.I. Molina, M. Fehrer, and D. Hommel, *J. Cryst. Growth* 216, 15 (2000).
10. A.M. Sanchez, F.J. Pacheco, S.I. Molina, J. Stemmer, J. Aderhold, and J. Graul, *Mater. Sci. Eng. B* (in press).
11. J.W. Matthews and A.E. Blakeslee, *J. Cryst. Growth* 27, 118 (1974).
12. E. Kasper and H.J. Herzog, *Thin Solid Films* 44, 357 (1977).
13. P.M.J. Marée, R.U. Olthof, J.W.M. Frenken, J.F. van der Veen, C.W.T. Bulle-Lieuwma, M.P.A. Viegers, and P.C. Zalm *J. Appl. Phys.* 58, 3097 (1985).
14. A. Fischer, H. Kühne, and H. Richter, *Phys. Rev. Lett.* 73, 2712 (1994).
15. J.L. Rouviere, M. Arley, B. Daudin, G. Feuillet, and O. Briot, *Mater. Sci. Eng. B* 50, 61 (1997).
16. C. Kim, I.K. Robinson, J. Myoung, K. Shim, M.-C. Yoo, and K. Kim, *Appl. Phys. Lett.* 69, 2358 (1996).
17. L. Sugiura, *J. Appl. Phys.* 81, 1633 (1997).
18. S. Ruminov, Z. Liliental-Weber, T. Suski, J.W. Ager III, J. Washburn, J. Drueger, C. Kisielowski, E.R. Weber, H. Amano, and I. Akasaki, *Appl. Phys. Lett.* 69, 990 (1996).